AIP | Journal of Applied Physics

Electromigration induced Kirkendall void growth in Sn-3.5Ag/Cu solder joints

Yong Jung and Jin Yu

Citation: Journal of Applied Physics **115**, 083708 (2014); doi: 10.1063/1.4867115
View online: http://dx.doi.org/10.1063/1.4867115
View Table of Contents: http://scitation.aip.org/content/aip/journal/jap/115/8?ver=pdfcov
Published by the AIP Publishing

Articles you may be interested in

Influence of Cu column under-bump-metallizations on current crowding and Joule heating effects of electromigration in flip-chip solder joints
J. Appl. Phys. **111**, 043705 (2012); 10.1063/1.3682484

Effects of Ag on the Kirkendall void formation of Sn–xAg/Cu solder joints
J. Appl. Phys. **108**, 083532 (2010); 10.1063/1.3488629

Electromigration induced high fraction of compound formation in SnAgCu flip chip solder joints with copper column
Appl. Phys. Lett. **92**, 262104 (2008); 10.1063/1.2953692

Effect of contact metallization on electromigration reliability of Pb-free solder joints
J. Appl. Phys. **99**, 094906 (2006); 10.1063/1.2193037

Electromigration failure mechanisms for SnAg 3.5 solder bumps on Ti Cr - Cu Cu and Ni (P) Au metallization pads
J. Appl. Phys. **96**, 4518 (2004); 10.1063/1.1788837

Re-register for Table of Content Alerts

Create a profile.

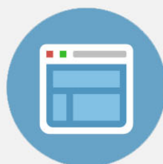

Sign up today!

[This article is copyrighted as indicated in the article. Reuse of AIP content is subject to the terms at: http://scitation.aip.org/termsconditions. Downloaded to] IP: 143.248.118.104 On: Wed, 21 May 2014 00:20:17

JOURNAL OF APPLIED PHYSICS 115, 083708 (2014)

Electromigration induced Kirkendall void growth in Sn-3.5Ag/Cu solder joints

Yong Jung and Jin Yu[a)]
Department of Materials Science and Engineering, Electronic Packaging Laboratory, KAIST, 373-1 Guseong-dong, Yuseong-gu, Daejeon 305-701, South Korea

(Received 6 December 2013; accepted 17 February 2014; published online 28 February 2014)

Effects of electric current flow on the Kirkendall void formation at solder joints were investigated using Sn-3.5Ag/Cu joints specially designed to have localized nucleation of Kirkendall voids at the Cu_3Sn/Cu interface. Under the current density of 1×10^4 A/cm^2, kinetics of Kirkendall void growth and intermetallic compound thickening were affected by the electromigration (EM), and both showed the polarity effect. Cu_6Sn_5 showed a strong susceptibility to the polarity effect, while Cu_3Sn did not. The electromigration force induced additional tensile (or compressive) stress at the cathode (or anode), which accelerated (or decelerated) the void growth. From the measurements of the fraction of void at the Cu_3Sn/Cu interface on SEM micrographs and analysis of the kinetics of void growth, the magnitude of the local stress induced by EM was estimated to be 9 MPa at the anode and −7 MPa at the cathode. © *2014 AIP Publishing LLC*.
[http://dx.doi.org/10.1063/1.4867115]

I. INTRODUCTION

In recent years, with the trend of chip miniaturization, electromigration (EM) damage of flip-chip solder joints has emerged as a serious reliability concern.[1–3] Solder bumps with the diameter of 50 μm are expected to operate under the current density of 10^4-10^5 A/cm^2, where electromigration in solder can lead to void formation at the joint and cause early failure of packages.[4] EM refers to the migration of atoms in response to an applied electric field by the momentum transfer between moving electrons and diffusing atoms. In metallic interconnects, EM force induces matter flux toward the anode building compressive (tensile) stress at the anode (cathode), which can lead to hillock (void) formation.[5] In the case of flip chip solder joints, EM can occur at much lower current density due to low critical product and the current crowding effect,[6] which leads to subsequent void formation and phase separation.[7] Variations of matter flux by EM affect intermetallic compound (IMC) thickening, and accelerated growth of Cu_6Sn_5 and Cu_3Sn were reported at the anode side in Sn-3.8Ag-0.7Cu/Cu system.[8]

Another reliability concern in the flip chip solder joints is Kirkendall void formation. Vacancy flux (J_v) caused by the nonreciprocal diffusive flux of atoms of different species induces tensile stress in the region of vacancy annihilation and compressive stress in the region of vacancy generation.[9–11] The presence of tensile stress is a necessary condition of void nucleation and growth. It must be provided either by external loading or by internal mechanisms. In Sn-3.5Ag/Cu solder joints, Yu and Kim[12] showed that the stress generated by the Kirkendall effect (KE) caused void nucleation in the Cu_3Sn matrix, but not nucleation at the Cu_3Sn/Cu interface. However, when the interface became embrittled by the segregation of residual S atoms, which originated from the bis-sodium sulfo-propyl-disulfide (SPS) additive to the electroplating solution, heterogeneous nucleation of voids could occur, which subsequently grew by the tensile stress evolving as a result of the KE. Since the magnitude of the stress generated at the Cu_3Sn/Cu interface depends on the magnitude of the net matter flux there and the efficiency of the interface as vacancy source/sinks, an application of EM force which induces additional matter flux is expected to change the local stress state and affect the kinetics of Kirkendall voiding.

Previous work on the coupling between EM and KE were more focused on the IMC growth than on voiding,[8,13–15] yet it is the latter which is truly detrimental from the standpoint of solder joint drop reliability. Recently, Liu *et al*. reported that localized Kirkendall voids in Cu/Sn/Cu flip chip joints formed only at the Cu_3Sn/Cu interface of the anode side and that voids did not form at the cathode side.[16] In the present work, the coupling between EM and KE was investigated using Sn-3.5Ag/Cu joints. Void nucleation was facilitated and controlled by adding a constant amount of SPS, a source of residual S in the Cu UBM, to the electroplating bath, and void growth was monitored by measuring the fraction of Kirkendall voids on the IMC/metal and IMC/IMC interfaces of solder joints with or without electric current application. Then, from the kinetics analyses of void growth, the magnitude of the tensile stress induced by KE and EM was estimated, and the polarity effect on the EM-induced stress was discussed.

II. EXPERIMENTAL PROCEDURE

A schematic diagram of the test vehicle used in the analysis is presented in Fig. 1 where Cu/Sn-3.5Ag/Cu solder joints were prepared by multiple reflows of Sn-3.5Ag solder balls, with a diameter of 350 μm, at 260 °C for 1 min, between the two PCBs which had 20 μm thick Cu openings (230 μm in diameter). Chemical composition of the electroplating bath was 1M $CuSO_4{\cdot}5H_2O$, 0.7M H_2SO_4, and 3.0×10^{-5}M SPS

a)jinyu@kaist.ac.kr

 © 2014 AIP Publishing LLC

[This article is copyrighted as indicated in the article. Reuse of AIP content is subject to the terms at: http://scitation.aip.org/termsconditions. Downloaded to] IP: 143.248.118.104 On: Wed, 21 May 2014 00:20:17

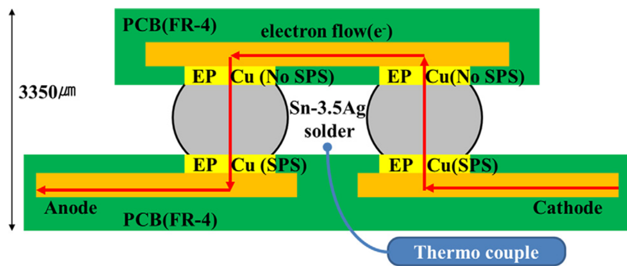

FIG. 1. A schematic diagram of the specimens used for the electromigration studies.

($C_6H_{12}O_6S_4Na_2$), and previous analysis showed that S content in the Cu UBM (analyzed by SIMS) and at the Cu_3Sn/Cu interface (analyzed by AES) were 16.8 ppm and 26%, respectively, with this level of SPS in the electroplating bath.[9,12] Ageing treatments were subsequently conducted at 150 °C up to 200 h with or without electricity application. The electric current flow was kept constant at 4.15 A which corresponded to the average current density of 1×10^4 A/cm^2 over the pad area. Temperature was kept constant at 150 °C by putting a thermocouple close to the solder ball connecting the chip and the substrate, thereby automatically taking into account the Joule heating effect caused by the current crowding. Kinetics of IMC thickening and Kirkendall voiding were analyzed from SEM micrographs taken from the solder joint area at the bottom PCB side, which was reflowed only once, as compared to the top PCB side which was reflowed twice. Underfill, which makes a mechanical support on the solder joint, was not filled in the gap between the PCBs in order to remove its effects. When Kirkendall voids did not cover the entire interface, line fractions of the interface voids were measured on SEM micrographs. When an interface was separated and opened up like an interfacial micro-crack, a cross-section of the micro-crack on SEM micrographs was used to estimate the crack opening, etc.

III. RESULTS

A. Content elemental analysis including S in Cu UBM using SIMS

As shown in Fig. 2, SIMS analysis was performed in order to know the contents of elements in the electroplated Cu UBM. Cu was electroplated using several electroplating baths on silicon wafer, which were sputtered with Ti and Cu, 100 nm each. Cu with a thickness of 20 μm was electroplated using electroplating solution with SPS added, as follows. 10 mg of SPS is an amount corresponding to 3.0×10^{-5}M, which was the same amount used in the experiments of Yu and Kim.[9,12] It is possible to know that as the content of SPS increased, the levels of S, C, O, and Cl were increased gradually. S, C, and O elements are essentially contained inside the SPS, and S is also contained in the electroplating solution because Cu sulfate and sulfuric acid are included in the bath. S is expected to be saturated even if excessive SPS was put in the bath.

B. IMC formation

Microstructures of the as-reflowed solder joint after the reflow (1 min at 260 °C) is given in Fig. 3(a), and it can be seen that Cu_3Sn IMC did not form at this stage and only scallop type Cu_6Sn_5 IMC formed at the joint interface. Note that Kirkendall voids did not form at the solder joint interfaces at this stage presumably because the equilibrium adsorption level of S at 260 °C was not significant enough to cause embrittlement or the equilibrium segregation was not reached due to the short reflow time.

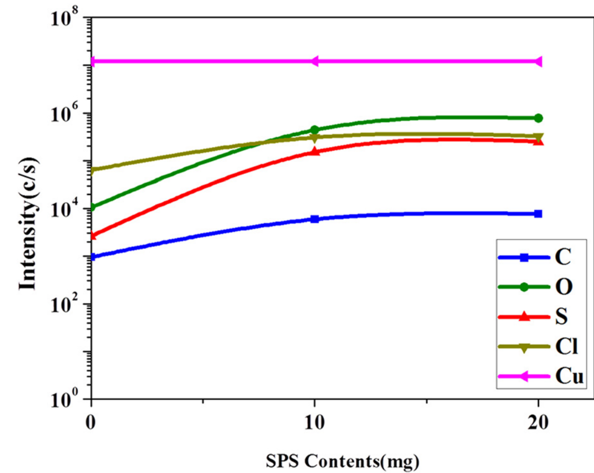

FIG. 2. Chemical compositions of the electroplated Cu film in thickness of 20 μm by SIMS according to SPS contents.

1. Ageing without electric current flow

Cross-sectional back scattered electron (BSE) images of Sn-3.5Ag/Cu joints at various stages ageing time after the reflow when electricity was not applied are presented in Fig. 3. It can be seen that the morphology of the Cu_6Sn_5 changed from scallop shape to the layer-type as a Cu_3Sn layer developed at the joint interface. After 60 h ageing at 150 °C, Kirkendall voids formed, mostly at the Cu_3Sn/Cu interface and a few in the Cu_3Sn matrix, but none at all in Cu_6Sn_5 or at any other interfaces. With further ageing, continuous nucleation and growth of voids and their coalescence at the Cu_3Sn/Cu interface made the interface fully covered with voids after around 100 h of ageing. As more Kirkendall voids formed at the Cu_3Sn/Cu interface, the relative magnitude of the Cu flux from the underlying UBM into Cu_3Sn diminished in comparison to that of Sn through the above Cu_6Sn_5 layer, thereby transforming Cu_3Sn into Cu_6Sn_5. As the voiding at the Cu_3Sn/Cu interface became severe and the Cu_3Sn/Cu_6Sn_5 transformation neared completion, diffusion of Sn atoms into the underlying Cu UBM through newly formed Cu_6Sn_5 formed a new Cu_3Sn layer below the initial Kirkendall void line. That was marked as the secondary IMC in Fig. 3(c). When the new Cu_3Sn/Cu interface became embrittled by the Gibbsian segregation of S, Kirkendall voids again formed there. The process can be repeated producing multiple Kirkendall void lines.[17,18]

In Fig. 4(a), IMC thickness is plotted as a function of the ageing time at 150 °C. It can be seen that the thickness of Cu_3Sn increased parabolically up to 100 h, decreased notably at 200 h, and then remained more or less constant afterwards. In the case of Cu_6Sn_5, IMC thickness increased rather linearly with the ageing time up to 100 h, but overall growth

[This article is copyrighted as indicated in the article. Reuse of AIP content is subject to the terms at: http://scitation.aip.org/termsconditions. Downloaded to] IP: 143.248.118.104 On: Wed, 21 May 2014 00:20:17

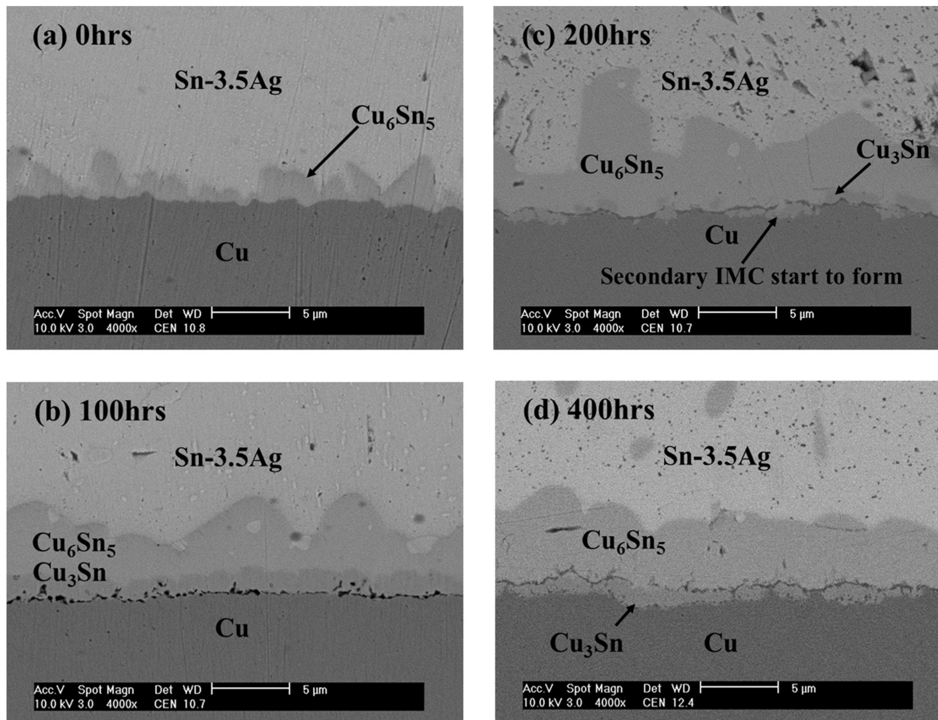

FIG. 3. Cross-sectional BSE images of Sn-3.5Ag/Cu solder joint aged at 150 °C without electricity flow for (a) 0 h, (b) 100 h, (c) 200 h, and (d) 400 h, respectively.

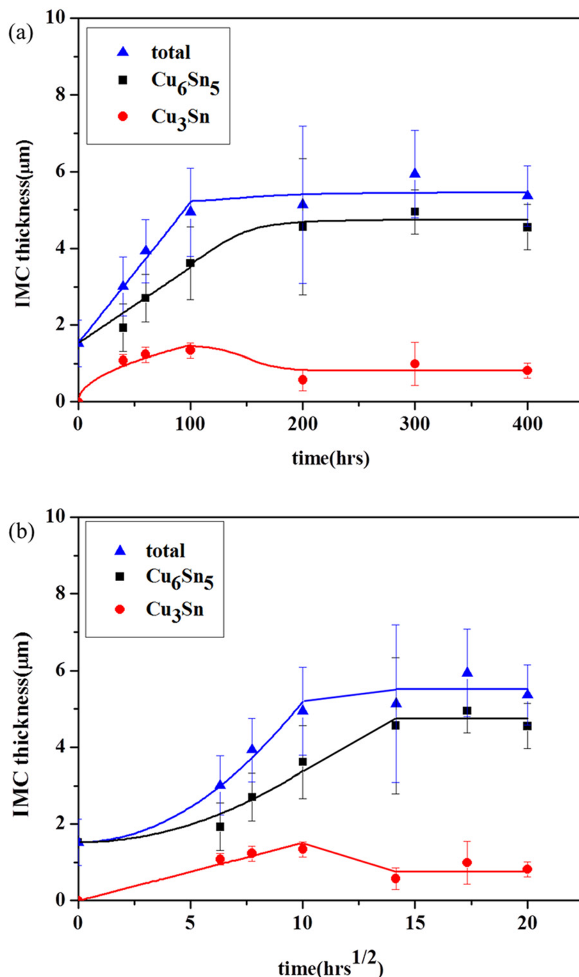

FIG. 4. Thickening of IMCs at 150 °C without electricity flow (a) according to time and (b) according to time$^{1/2}$.

kinetics up to 200–300 h can be better described by the parabolic growth.

In the diffusion-controlled layer growth mechanism proposed by Kidson,[19] kinetics of IMC growth is described by

$$\delta - \delta_0 = \alpha t^{\frac{1}{2}}, \quad (1)$$

where δ_0 is the IMC thickness of the as-reflowed condition and α is a constant which is related to the interdiffusivities of the two phases adjoining the interface. However, if the kinetics is related to the interface reaction controlled growth mechanism, the kinetics would follow:

$$\delta - \delta_0 = \beta t. \quad (2)$$

Thus, examining whether the IMC thickening shows better fit with the parabolic or linear time scale is a measure of the IMC growth mechanism. In the Sn-3.5 Ag/ Cu joints, it is well established that thickening of both Cu_3Sn and Cu_6Sn_5 is better described by Eq. (1), which occurs by the diffusion controlled layer growth mechanism.[9,12,18] In that context, the present result is not consistent with the previous work.

The discrepancy in the IMC growth kinetics between the present work and others can be ascribed to abnormalities associated with the Kirkendall voiding and the secondary IMC formation. Severance of Cu influx from the underlying UBM by the nucleation of Kirkendall voids at the Cu_3Sn/Cu interface and subsequent transformation of Cu_3Sn into Cu_6Sn_5 eventually made δ_{Cu3Sn} to diminish after 100 h. Was it not for the Kirkendall voiding, the kinetics of Cu_6Sn_5 thickening would show the parabolic growth mode; however, the additional formation of Cu_6Sn_5 by the dissolution of Cu_3Sn caused δ_{Cu6Sn5} deviate from the parabolic to near-linear growth. IMC thicknesses reported in this work are somewhat smaller than those of other workers. Possibilities

[This article is copyrighted as indicated in the article. Reuse of AIP content is subject to the terms at: http://scitation.aip.org/termsconditions. Downloaded to] IP: 143.248.118.104 On: Wed, 21 May 2014 00:20:17

include variations of actual solder joint temperature due to Joule heating and the effects of interfacial Kirkendall voids reducing the matter flux across the interface.

2. Ageing under the electric current density of 1×10^4 A/cm^2

When solder joints are subjected to electricity flow during the ageing treatment, the kinetics of IMC thickening are affected due to the additional matter flow driven by the EM force, which depends on the current density and the polarity.[8] Cross-sectional SEM micrographs of the solder joint aged at 150 °C under the electric current density of 1×10^4 A/cm^2 are presented in Figs. 5 and 6. It can be seen that EM exerted the polarity effect not only on the IMC thickening but also on the Kirkendall voiding. With the application of the electric current, both IMC growth and Kirkendall voiding were accelerated at the anode side, but decelerated at the cathode side.

The polarity in the IMC thickening came mostly from that of Cu_6Sn_5. The thickness of Cu_3Sn was smaller than that of Cu_6Sn_5 in general and did not show much polarity. That is basically consistent with the reports by Gan and Tu[8] and Chao *et al.*[20] If the growth of Cu_3Sn occurred by the diffusion controlled mechanism described by Eq. (1), values of α, which was $0.15 \pm 0.02\,\mu$m/h$^{1/2}$ ($t < 100$ h) without EM became 0.16 ± 0.03 and $0.1 \pm 0.05\,\mu$m/h$^{1/2}$ for the anode and cathode as shown in Figs. 4(b), 7(b), and 8(b), respectively. In the case of Cu_6Sn_5, α was $0.19 \pm 0.04\,\mu$m/h$^{1/2}$ without EM but changed to 0.52 ± 0.09 and $0.13 \pm 0.05\,\mu$m/h$^{1/2}$ for the anode and cathode, respectively. Values of α reported by other workers[14,21] were 0.15 and 0.33 for Cu_3Sn and Cu_6Sn_5, respectively, when there was no EM. It can be seen that Cu_6Sn_5 grew much faster than Cu_3Sn ($\alpha_{Cu_6Sn_5} \sim 2\alpha_{Cu_3Sn}$), if it was not for the Kirkendall void formation.

When electricity is applied, the kinetics of IMC growth was still diffusion-controlled at the cathode, but not so at the anode side. At the cathode side, it can be seen that the thickening of Cu_3Sn was not much affected by EM, but that was not true of Cu_6Sn_5. In fact, Cu_6Sn_5 did not thicken at all, as shown in Fig. 6(a). Presumably, that was related to the early separation of the Cu_6Sn_5/Sn interface and subsequent separation of Cu/Cu_3Sn interface, which blocked the material flow necessary to feed further IMC growth, in Fig. 6(d).

Characteristics of IMC thickening at the anode side were different from those at the cathode side or those of solder joints in the absence of the electric current flow. Here, interface separation did not occur and the IMC thickening changed over to a reaction-controlled growth, which can be described as Eq. (2).

From Fig. 7, it can be seen that the accelerated IMC growth at the anode can be ascribed to Cu_6Sn_5 ($\beta_{Cu_6Sn_5} \sim 3\beta_{Cu_3Sn}$). The transition in the IMC growth mode was driven by the EM flow which was proportional to time (see next), and the trend is consistent with the observations of other workers.[13,14,20]

C. Kirkendall voiding

In addition to the polarity effect on the IMC thickening, EM was found to affect Kirkendall voiding at the solder joints as well, however, in a way quite different from those reported by Liu *et al.*[16] In Figs. 5 and 6, SEM micrographs out of the anode and cathode parts of the solder joints are presented, respectively, at several ageing times. It can be seen that Kirkendall voiding at the Cu/Cu_3Sn interface was accelerated at the anode and was suppressed at the cathode by EM, as compared to the case without current, and details can be described by the following.

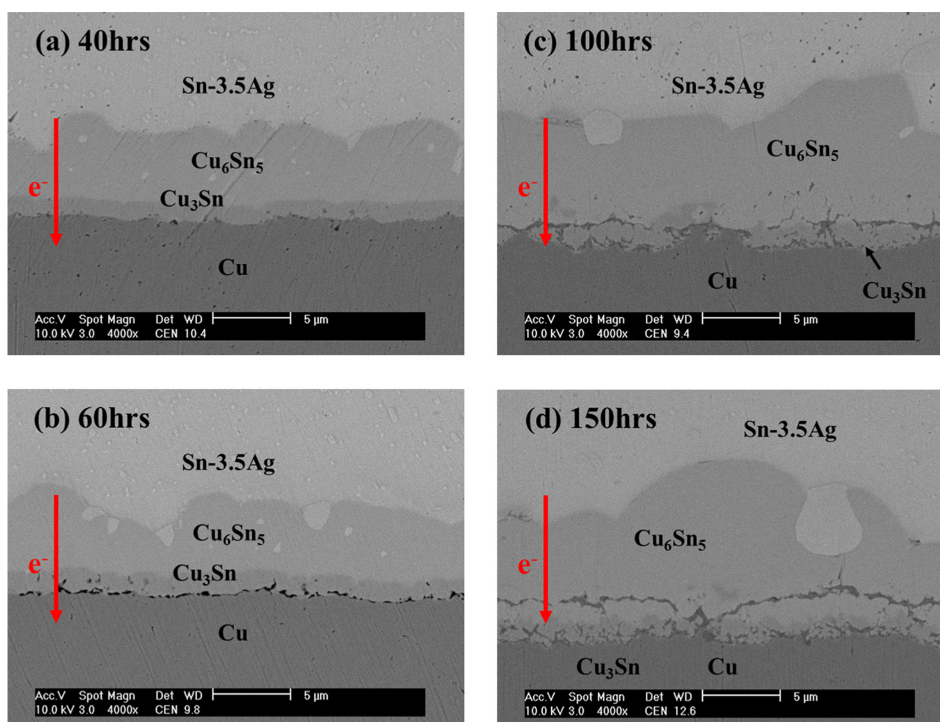

FIG. 5. Cross-sectional BSE images of Sn-3.5Ag/Cu joints aged at 150 °C under the electric current density of 1×10^4 A/cm^2 at the anode side after (a) 40 h, (b) 60 h, (c) 100 h, and (d) 150 h, respectively.

[This article is copyrighted as indicated in the article. Reuse of AIP content is subject to the terms at: http://scitation.aip.org/termsconditions. Downloaded to] IP: 143.248.118.104 On: Wed, 21 May 2014 00:20:17

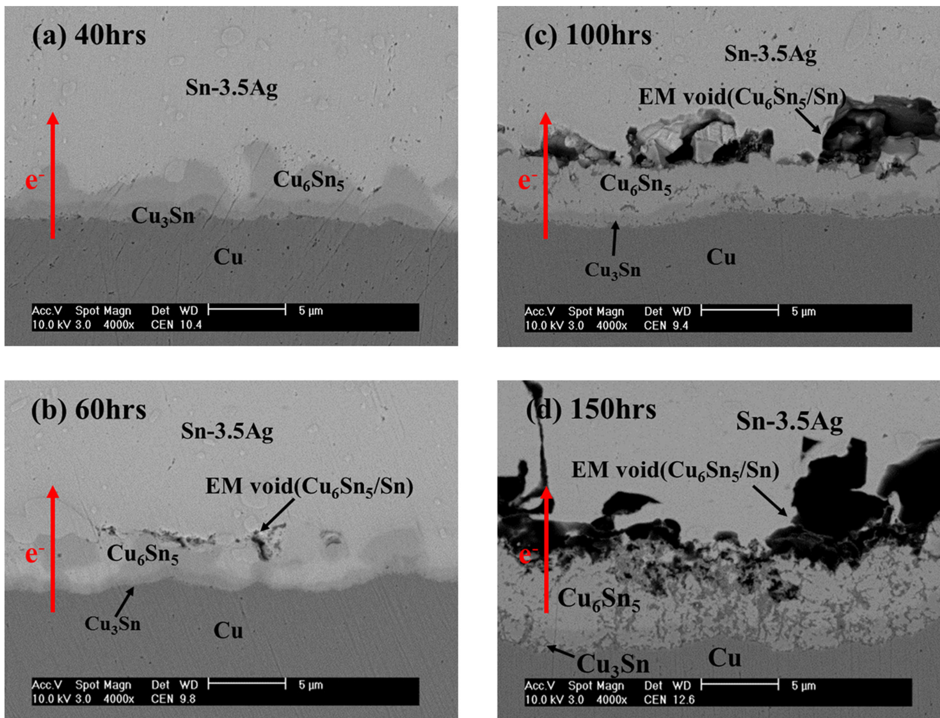

FIG. 6. Cross-sectional BSE images of Sn-3.5Ag/Cu joints aged at 150 °C under the electric current density of 1×10^4 A/cm^2 at the cathode side after (a) 40 h, (b) 60 h, (c) 100 h, and (d) 150 h, respectively.

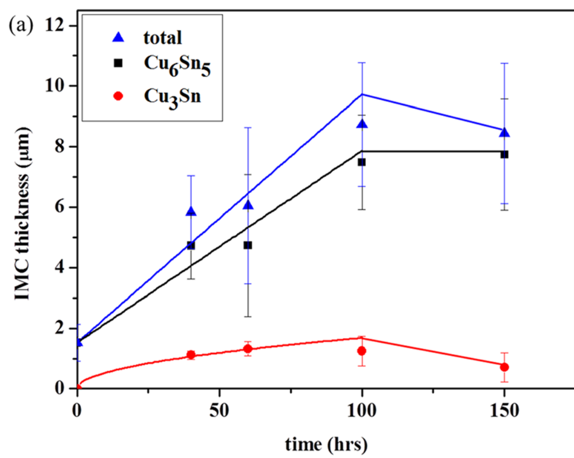

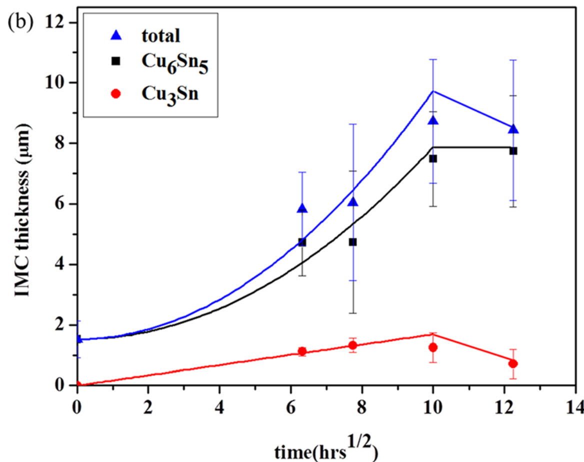

FIG. 7. Thickening of IMCs at 150 °C under the electric current density of 1×10^4 A/cm^2 at the anode side (a) according to time and (b) according to time$^{1/2}$.

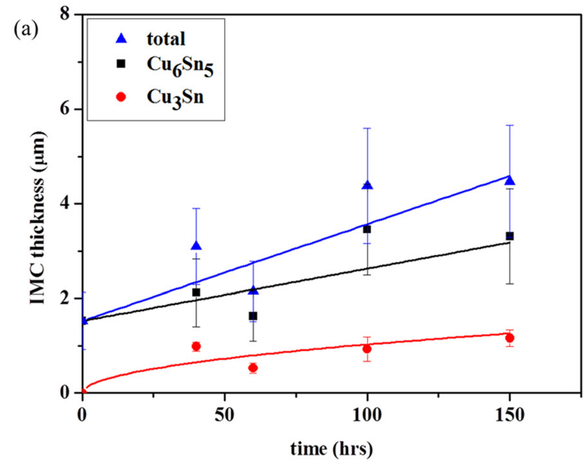

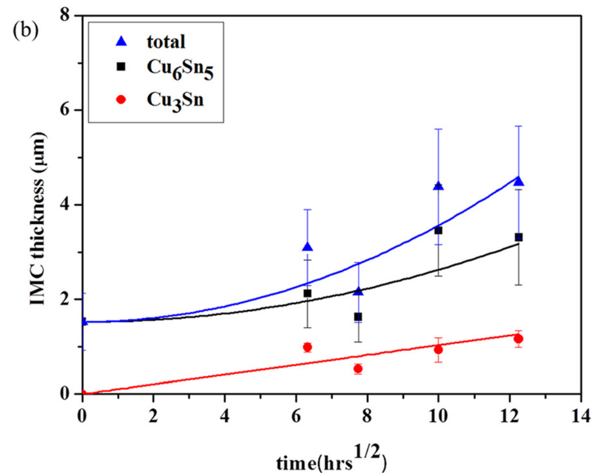

FIG. 8. Thickening of IMCs at 150 °C under the electric current density of 1×10^4 A/cm^2 at the cathode side (a) according to time and (b) according to time$^{1/2}$.

[This article is copyrighted as indicated in the article. Reuse of AIP content is subject to the terms at: http://scitation.aip.org/termsconditions. Downloaded to] IP: 143.248.118.104 On: Wed, 21 May 2014 00:20:17

(1) At the anode side, Kirkendall voids initially formed at the Cu/Cu_3Sn interface (cf. 40 h) and occupied a large portion of the interface at 60 h. And after 100 h, the interface was separated almost linearly. And then IMCs and Cu were reacted again, and the secondary IMCs were formed under the separated interface.
(2) At the cathode side, Kirkendall voids formed and occupied a large fraction of the Cu/Cu_3Sn interface at 100 h and almost saturated the interface after 150 h. A completely new development began around 100 h. The Cu_6Sn_5/Sn interface became separated by EM and started to form micro-cracks larger than 10 μm in length. The scale of the damage on the Cu_6Sn_5/Sn interface was much more severe than that on the Cu/Cu_3Sn interface caused by Kirkendall voids. The micro-cracks eventually interlinked and formed macro-cracks, covering the whole joint area after 150 h.

Characteristics of Kirkendall void formation at the Cu/Cu_3Sn interface of the solder joints with or without EM are presented in Fig. 9 where the line fractions covered by voids (L) are plotted as a function of the ageing time. Without the electricity application, Kirkendall voids fully covered the Cu/Cu_3Sn interface after 100 h of ageing at 150 °C. Those were lower at the cathode side of the solder joint when the electricity with current density of 10^4 A/cm^2 was applied. The kinetics became somewhat slower and the full coverage of the interface by voids occurred at 150 h. However, at the anode side, Kirkendall voids nucleated and grew at the Cu/Cu_3Sn interface faster than without the electricity.

IV. DISCUSSION

A. Effects of EM on the Kirkendall voiding

EM force pushes atoms toward the anode creating compressive stress there, which can be subsequently relaxed by creep. In the case of a eutectic Sn-3.5Ag solder joint, the ageing temperature is above 0.8 T_m, and the stress can be readily relaxed by Nabarro-Herring and/or dislocation creep

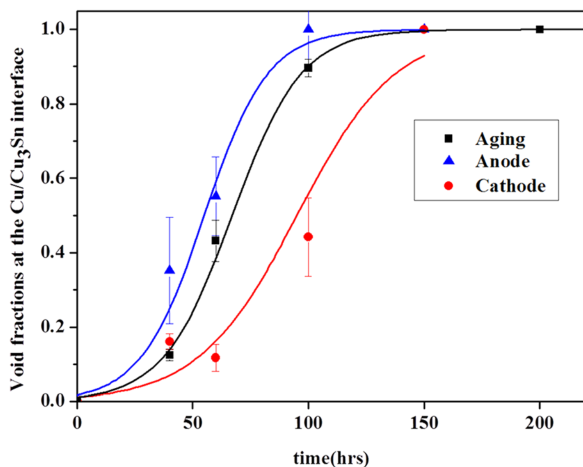

FIG. 9. The line fraction of Kirkendall voids at Cu/Cu_3Sn interface as a function of ageing time at 150 °C under anodic, cathodic and w/o current conditions.

mechanisms.[22] In contrast, the ageing temperature is below 0.4 T_m for Cu pad or IMCs and the creep is not fast enough to relax these stresses completely and elastic strain dominates. Under a steady state situation, local tensile stress is maintained at a certain level which is the results of Kirkendall effect, electromigration, and the creep relaxation. They all add up. The EM-induced stress in the region decreases the Kirkendall stress by the principle of superposition and affects Kirkendall void nucleation and growth.

One way to estimate the EM-induced stress is to analyze the Kirkendall void growth rate. In the case of quasi-equilibrium growth of Kirkendall voids, the void growth rate, presented in terms of the line fraction of voids (L) at the Cu_3Sn/Cu interface, can be written as[18,23]

$$\dot{L} = \frac{D_B \delta_B \Omega}{hkTb^3L^2} \cdot \frac{\sigma_{yy} - (1-L^2)\sigma_0}{\left\{-2\ln(L) - \frac{1}{2}(3-L^2)(1-L^2)\right\}}, \quad (3)$$

where L is defined as the ratio between the void radius (a) and the inter-void half spacing (b) and D_B, δ_B, Ω, h, k, T, and σ_{yy} refer to the grain boundary diffusivity of copper, and the grain boundary thickness of copper, atomic volume, geometrical constant of void, Boltzmann constant, Temperature, and normal stress to the interface, respectively ($\delta_B D_B = 4.0\times10^{-26}$ m^3/s,[24] $a = 10^{-8}$ m, $b = 2.1\times10^{-7}$ m, $h = 0.775$). The sintering stress σ_0 is defined as $\frac{2f}{a}$ where f is the surface stress of Cu at 150 °C. Since the value of surface stress was not available, the sintering stress term was ignored in the present analysis. In Eq. (3), instantaneous nucleation of voids upon loading was tacitly assumed and the deduction of σ_{yy} from the $\dot{L}$ measurement was done at large L; for example, 0.5 in the case of the anode side, which involved less error.

From the measurement of $\dot{L}$ at $L = 0.5$, the magnitude of local tensile stress at the Cu_3Sn/Cu interface in the case of applying current for 60 h which drove the void growth was estimated to be 38 MPa at the anode side. The tensile stress estimated for the cathode and w/o current sides by the same method were 22 and 29 MPa, respectively. These are underestimated values considering the fact that the inter-void spacing b decreased with L in the case of continual nucleation of voids. Since the local tensile stress was the sum of Kirkendall and EM-induced stresses, the difference between the stress at the anode and that at the w/o current electrode was ascribed to the EM force at the anode. That was estimated to be 9 MPa at the anode (−7 MPa at the cathode) at the Cu_3Sn/Cu interface.

B. An elastic/plastic analysis of the coupled stress which drives the Kirkendall void growth

Internal stresses of electroplated Cu film with various copper sulfate baths have a range of −41 MPa to 54 MPa.[25] Negative value indicates a compressive stress. This value changes according to the bath conditions and several other additives. Zhou *et al.*[26] measured residual stress of the electroplated copper films by nanoindentation which was estimated to be 19.3 MPa. In previous analysis on the Kirkendall void growth,[12] Yu and Kim calculated σ_{res} of electroplated

[This article is copyrighted as indicated in the article. Reuse of AIP content is subject to the terms at: http://scitation.aip.org/termsconditions. Downloaded to] IP: 143.248.118.104 On: Wed, 21 May 2014 00:20:17

Cu film on the Si wafer by measuring the wafer curvature with laser scanning. The estimated residual stress values of electroplated Cu films were all tensile, 55 MPa without SPS, and increased linearly with the SPS content.

It was suggested that tensile stress can develop at the Cu_3Sn/Cu interface as vacancies annihilate there to meet the condition of matter flux continuity. If the interface is an ideal source/sink of vacancies and vacancies are generated there with a rate $\dot{N}$ (per unit area per unit time), the evolution of strain at the interface can be described by

$$\dot{\varepsilon}_{yy} = -\frac{\Omega \dot{N}}{L}, \tag{4}$$

where L is an arbitrary length scale taken to be the solder joint height (=$L_0 + L_1 + L_2 + L_S$, each denoting thickness of Cu UBM, Cu_3Sn, Cu_6Sn_5, and solder, respectively). The coordinate system has its origin at the original Cu/solder interface before reflow and extends into the solder, which is a laboratory coordinate system.

The vacancy generation rate at the interface is related to the vacancy flux (J_v) and maker velocity (v_i) of adjoining phases by

$$\Omega \dot{N} = \Omega\left\lfloor (J_v)_{Cu_3Sn} - (J_v)_{Cu} \right\rfloor = v_{Cu_3Sn} - v_{Cu}. \tag{5}$$

In a binary stoichiometric compound, the marker velocity by KE was approximated as[27]

$$v_{KE} = \frac{\dfrac{D_{Cu}}{D_{Sn}} - 1}{\left(\dfrac{D_{Cu}}{D_{Sn}}\right) N_{Sn} + N_{Cu}} \left(\frac{\tilde{D}_{\text{int}}}{\Delta x}\right), \tag{6}$$

where N_i is mole fraction, D_i is intrinsic diffusivity, $\tilde{D}_{\text{int}}$ is integrated diffusivity, and Δx is IMC thickness. $\tilde{D}_{\text{int}}$ is approximated as $\tilde{D}\Delta N$ where $\tilde{D}$ is interdiffusivity and ΔN is the variance of N_{Cu} in the Cu_3Sn layer. Calculations of the marker velocity using Eq. (6) and materials parameters listed in Table I and Refs. 13, 14, and 20 give positive $\dot{\varepsilon}_{yy}$ (and $\dot{\sigma}_{yy}$) for the Cu_3Sn/Cu interface but negative $\dot{\varepsilon}_{yy}$ (and $\dot{\sigma}_{yy}$) for the Cu_6Sn_5/Cu_3Sn interface, which is qualitatively consistent with the experimental observation of Kirkendall voiding only at the Cu_3Sn/Cu interface.

As vacancies annihilate at the interface continually, local tensile stress increases with time, but the evolving stress soon reached a steady state value by the elastic/plastic response of the solder joint. Since depletion of lattice planes at the interface under the constrained displacement condition is equivalent to elongation of the joint at the same speed, the constitutive equation of the solder joint can be written as follows:

$$B\sigma_{yy}^n + \frac{\dot{\sigma}_{yy}}{E} = -\frac{\Omega \dot{N}}{L_S} = -\frac{(v_{Cu_3Sn} - v_{Cu})}{L_S}. \tag{7}$$

Here, the Cu UBM and IMCs were assumed to remain elastic while the solder underwent power law creep deformation ($\dot{\varepsilon} = B\sigma^n$) during the process. The average Reuss modulus of the joint E is defined by[18]

$$E = \left(\frac{L_{Cu}}{L_S}\frac{1}{E_{Cu}} + \frac{L_1}{L_S}\frac{1}{E_1} + \frac{L_2}{L_S}\frac{1}{E_2}\right)^{-1}. \tag{8}$$

Under the application of electric current, the marker movement is affected by the KE and EM simultaneously and the corresponding marker velocity can be written as

$$v = v_{KE} + v_{EM}. \tag{9}$$

The marker velocity induced by EM is given by

$$v_{EM} = \Omega J_v^{EM} = -\Omega\left[\left(J_{Cu}^{EM}\right) + \left(J_{Sn}^{EM}\right)\right], \tag{10}$$

where J_v^{EM}, J_{Cu}^{EM}, and J_{Sn}^{EM} denote vacancy and matter fluxes induced by EM force, respectively. The matter flux term on the RHS of Eq. (10) is given by

$$J_{Cu}^{EM} + J_{Sn}^{EM} = \frac{ej}{\Omega kT}\left(N_{Cu}D_{Cu}Z_{Cu}^*\rho_{Cu} + N_{Sn}D_{Sn}Z_{Sn}^*\rho_{Sn}\right) + \frac{1}{kT}\frac{d\sigma}{dx}\left(N_{Cu}D_{Cu} + N_{Sn}D_{Sn}\right), \tag{11}$$

where Z_i^*, e, ρ_i, and j refer to the effective charge number of EM, charge of an electron, resistivity, and the current density, respectively. The first term on the RHS of Eq. (11) refers to matter flux by EM force and the second term refers to backward matter diffusion induced by the stress gradient. The latter is a stress relaxation process by the Nabarro-Herring creep. If the stress gradient terms in Eq. (11) can be ignored, v_{KE} and v_{EM} in Cu_3Sn were estimated to be -2.93×10^{-12} m/s and -2.69×10^{-12} m/s in the case of aging and EM for 60 h, respectively, using material parameters except diffusivities given by Chao *et al.*[14] An extension of the above analysis to Cu_6Sn_5 gave $v_{KE} = 7.40 \times 10^{-13}$ m/s in the case of aging for 100 h and $v_{EM} = -4.16 \times 10^{-12}$ m/s in Cu_6Sn_5.

Equation (7) can be solved numerically to give the evolution of stress with time. A simple asymptotic analysis shows that σ_{yy} reaches a steady state value[18]

$$\sigma_{yy} = \left[\frac{-v_{Cu_3Sn} + v_{Cu}}{BL_S}\right]^{\frac{1}{n}}. \tag{12}$$

Calculated σ_{yy} values using relevant creep constants were 18 MPa at the cathode and 12 MPa at the anode side for the Cu_3Sn/Cu interface, respectively. And −14 MPa was deduced for the Cu_6Sn_5/Cu_3Sn interface at both sides. Here, it is very important use relevant creep constants, as creep

TABLE I. Diffusion coefficients derived by the void and stress propensities at the interfaces.

Phase	Diffusive species	D (m^2/s)	D_{inter} (m^2/s)
Cu_3Sn	Cu	5.12×10^{-16} (Ref. 35)	2.38×10^{-16}
	Sn	1.46×10^{-16} (Ref. 35)	
Cu_6Sn_5	Cu	1.50×10^{-16}	2.86×10^{-16}
	Sn	4.0×10^{-16}	

[This article is copyrighted as indicated in the article. Reuse of AIP content is subject to the terms at: http://scitation.aip.org/termsconditions. Downloaded to] IP: 143.248.118.104 On: Wed, 21 May 2014 00:20:17

data of solders vary widely with the microstructure and the stress state.[28] Creep constants used in the analysis were $B = 8 \times 10^{-17}(\text{MPa})^{-8.9}$/s and $n = 8.9$, which were obtained from the tensile creep testing of solders with the same composition and microstructure as the one shown in Fig. 2.[29] The stress calculated by Eq. (12) is a lower bound estimate because the tensile stress becomes more localized near the Cu_3Sn/Cu interface as Kirkendall voids grow.

However, the deduced stresses under EM were ignored the back stress gradient in Eq. (11). Thus, the estimated stresses have typical values in EM condition which the vacancies tend to move in the opposite direction of electron flow. The flux calculation from Gan and Tu,[8] which were assumed that Cu/Sn IMC as a single phase (Cu_6Sn_5), was expanded as dual IMCs (Cu_6Sn_5 and Cu_3Sn) conditions in order to consider the back stress gradient term. The back stress was estimated −5 MPa at the cathode and 10 MPa at the anode side for the Cu_3Sn/Cu interfaces in the case under EM for 60 h. As a result of the summation with the back stress and EM induced stress, σ_{yy} for the 60 h could be estimated as 13 MPa at the cathode and 21 MPa at the anode under EM compared to the 15 MPa in the isothermal ageing conditions.

It is interesting to note that the σ_{yy} value obtained by the elastic/plastic analysis is about the same order as that measured from the kinetics analysis of Kirkendall void growth. Considering the presence of residual stress introduced in the Cu UBM during the electroplating process, the agreement is reasonable.

For the calculation of v_{KE}, v_{EM}, and the stress analysis, the intrinsic diffusivities of Cu and Sn in each IMC, which determined the flux ratio and the dominant diffusive species in the IMCs, are critical parameter. There are still ambiguities in the diffusivities in Cu/Sn IMCs as follows. Onishi and Fujibuchi[30] reported that the Sn is more mobile than the Cu atom in Cu_6Sn_5. Tu and Thompson[31] reported that the Cu is dominant diffusing species in Cu_6Sn_5 IMC. Kumar *et al.*[32] concluded that Cu is a faster diffusing element than Sn in Cu_3Sn and Cu_6Sn_5. From the deduced diffusion coefficients by Chao *et al.*,[13,14] diffusive matter flux ratios can be obtained as follows, $|J_{Sn}| \sim 6.4\,|J_{Cu}|$ in Cu_3Sn and $|J_{Sn}| \sim 0.92\,|J_{Cu}|$ in Cu_6Sn_5,[13] $|J_{Sn}| \sim 7.97\,|J_{Cu}|$ in Cu_3Sn and $|J_{Sn}| \sim 1.1\,|J_{Cu}|$ in Cu_6Sn_5.[14] In this case, the Sn is a faster diffusive element in Cu_3Sn and matter fluxes moves in almost the same velocity in Cu_6Sn_5. Using these flux ratios, compressive stress can occur at the Cu/Cu_3Sn interfaces and tensile stress at the Cu_3Sn/Cu_6Sn_5 and Cu_6Sn_5/Sn interfaces during thermal ageing and at the cathode side under EM. They also reported that the dominant failure of the solder joints occurred at the Cu_6Sn_5 phase near the Cu_3Sn/Cu_6Sn_5 interface under high current stressing. This result is contradictory to our results. No voids were observed at the interfaces at the Cu_3Sn/Cu_6Sn_5 at both sides under EM and thermal ageing condition in this research.

Paul *et al.*[33] reported that $|J_{Sn}| \sim 0.9\,|J_{Cu}|$ in Cu_3Sn and $|J_{Sn}| \sim 1.6\,|J_{Cu}|$ in Cu_6Sn_5. It means that Cu is a faster diffusive element in Cu_3Sn and Sn is a faster diffusive element in Cu_6Sn_5. This tendency is well agreed with our void propensity results in the ageing cases. In that case, the void propensity could be explained that the Cu/Cu_3Sn and Cu_6Sn_5/Sn interfaces acted as vacancy sinks, while the Cu_3Sn/Cu_6Sn_5 interface acted as a source, and Kirkendall voids were not found at the Cu_6Sn_5/Sn interface because of absence of the S segregation. But no knowledge of individual tracer or activation energy was noticed at all. Paul *et al.*[34] also determined the tracer diffusion coefficient, the integrated diffusion coefficients and the activation energy for the Cu_3Sn and Cu_6Sn_5. They reported that $|J_{Sn}| \sim 0.033\,|J_{Cu}|$ in Cu_3Sn and $|J_{Sn}| \sim 2.38\,|J_{Cu}|$ in Cu_6Sn_5, but their diffusivities are less about a hundred times.

The intrinsic diffusivities in the IMCs which corresponded with our void propensity result under EM and thermal ageing conditions were deduced as presented in Table I. The diffusivities in Cu_3Sn from Wang[35] were well agreed with our results.

As shown in Fig. 10(b), compared to Kirkendall voiding at Cu/Cu_3Sn as presented in Fig. 10(a), EM-induced void growth at Cu_6Sn_5/Sn-3.5Ag solder interface at the cathode side is larger and may cause severe damage to the reliability of the solder joint. This void growth was shown only at the cathode side. The high applied current may cause the voiding failure at the solder/IMC interface. Calculated σ_{yy} at the Cu_6Sn_5/Sn-3.5Ag solder interface was 8 MPa at the cathode side and −7 MPa at the anode side. This shows that the tensile stress induced by EM caused the void growth at the cathode and the compressive stress reduced the void at the anode at the Cu_6Sn_5/Sn-3.5Ag solder interface, respectively. This is reasonably consistent with the result by Gan and Tu.[8] Their back stresses in the IMCs, which are interpolated according to the polarity for the same current density of

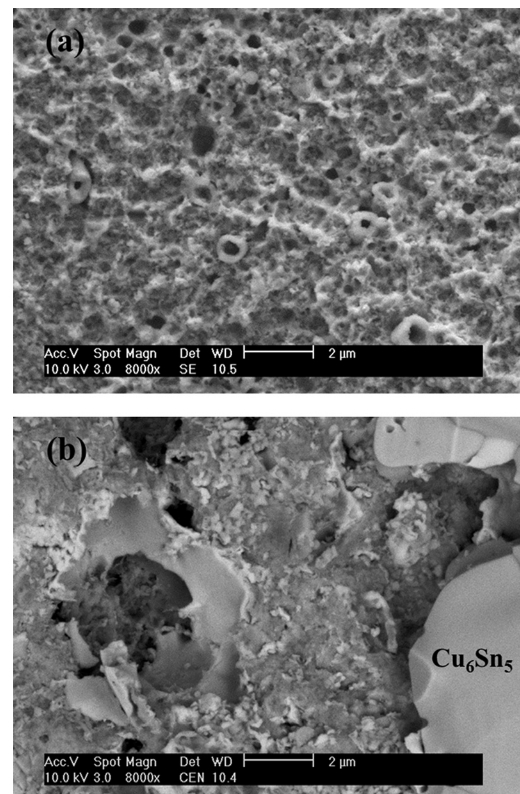

FIG. 10. Fractured joint surface after 200 h under the electric current density of 1×10^4 A/cm^2 (a) at the anode side and (b) at the cathode side, respectively.

[This article is copyrighted as indicated in the article. Reuse of AIP content is subject to the terms at: http://scitation.aip.org/termsconditions. Downloaded to] IP: 143.248.118.104 On: Wed, 21 May 2014 00:20:17

$1 \times 10^4\,\mathrm{A/cm^2}$, are estimated as -4.2 MPa at the anode and the 9 MPa at the cathode side, respectively. The EM induced stress is the difference of the stress at both sides so the total magnitude of stress is 13.2 MPa. This is consistent with the result in this work, EM induced stress is 15 MPa through the solder joint under a high current density condition.

Furthermore, Budiansky *et al.*[36] investigated the spherical voids growth in non-linear material under axisymmetric loading. And Hill[37] established the constitutive equations of the nonlinear viscous material. He and Hutchinson[38] also investigated the volume growth of a penny-shaped crack under the uniaxial tension condition. The simple approximation formula, which is valid to within 35% in uniaxial tension for all void shapes between a sphere and a crack, is as below

$$\Lambda = \frac{\dot{V}}{\dot{\varepsilon}\left(\frac{4}{3}\pi R^3\right)} = 1.1, \quad (13)$$

where $\dot{\varepsilon}$ is the tensile strain rate.

Assuming that the large micro-void at the Cu_6Sn_5/Sn-3.5Ag solder interface at the cathode side is a penny-shaped crack, and uniaxial tension is loaded on Sn-3.5Ag solder, the strain rate is equal to the strain rate by creep relaxation ($\dot{\varepsilon} = B\sigma^n$) of the solder, the stress on the Cu_6Sn_5/Sn-3.5Ag solder interface can be deduced to be 16 MPa. Thus, this value could be considered as the EM-induced stress through the solder joint as well.

V. CONCLUSIONS

Preferential Kirkendall void growth at the Cu_3Sn/Cu interface was induced by adding a constant amount of SPS to the electroplating bath of Cu which was a main source of S segregation at the interface. Application of the electric current showed the polarity effect in IMC and Kirkendall void growth in a different way. Cu_6Sn_5 showed strong polarity effect while Cu_3Sn did not. Both Cu_6Sn_5 and Kirkendall void were enhanced at the anode but suppressed at the cathode. From the analysis of Kirkendall void growth, tensile stress imposed by EM at the Cu_3Sn/Cu interface was estimated to be 9 MPa at the anode side, and compressive stress was estimated to be -7 MPa at the cathode side under the applied current density of $1 \times 10^4\,\mathrm{A/cm^2}$. Finally, an elastic/-plastic analysis of the IMC/solder joint was provided to estimate the tensile stress generation at the Cu_3Sn/Cu interface by vacancy annihilation under high current stressing.

ACKNOWLEDGMENTS

This work was supported by the National Research Foundation of Korea (NRF) grant funded by the Korea government (MEST) (No. 2013003834).

[1] T. Y. Lee, K. N. Tu, and D. R. Frear, J. Appl. Phys. **90**(9), 4502 (2001).
[2] Y. H. Lin, Y. C. Hu, C. M. Tsai, C. R. Kao, and K. N. Tu, Acta Mater. **53**(7), 2029 (2005).
[3] E. C. C. Yeh, W. J. Choi, K. N. Tu, P. Elenius, and H. Balkan, Appl. Phys. Lett. **80**(4), 580 (2002).
[4] The International Technology Roadmap for Semiconductors, Semiconductor Industry Association, 2007.
[5] I. A. Blech and C. Herring, Appl. Phys. Lett. **29**(3), 131 (1976).
[6] C. Chen, H. M. Tong, and K. N. Tu, Annu. Rev. Mater. Res. **40**, 531 (2010).
[7] K. N. Tu, "Solder joint technology," in *Materials, Properties, and Reliability* (Springer, 2007).
[8] H. Gan and K. N. Tu, J. Appl. Phys. **97**, 063514 (2005).
[9] J. Y. Kim and J. Yu, Appl. Phys. Lett. **92**, 092109 (2008).
[10] P. Shewmon, *Diffusion in Solids*, 2nd ed. (The Minerals, Metals and Materials Society, Warrendale, PA, 1989).
[11] M. E. Glickman, *Diffusion in Solids, Field Theory, Solid State Principles, and Applications* (A Wiley-interscience Publication, John Wiley & Sons, New York, 2000).
[12] J. Yu and J. Y. Kim, Acta Mater. **56**, 5514 (2008).
[13] B. Chao, S. H. Chae, X. Zhang, K. H. Lu, J. Im, and P. S. Ho, Acta Mater. **55**, 2805 (2007).
[14] B. Chao, S. H. Chae, X. Zhang, K. H. Lu, M. Ding, J. Im, and P. S. Ho, J. Appl. Phys. **100**, 084909 (2006).
[15] H. T. Orchard and A. L. Greer, Appl. Phys. Lett. **86**(23), 231906 (2005).
[16] C. Y. Liu, J. T. Chen, Y. C. Chuang, L. Ke, and S. J. Wang, Appl. Phys. Lett. **90**, 112114 (2007).
[17] S. H. Kim and J. Yu, J. Mater. Res. **25**(9), 1854 (2010).
[18] J. Y. Kim, J. Yu, and S. H. Kim, Acta Mater. **57**(17), 5001 (2009).
[19] K. N. Tu, J. W. Mayer, and L. C. Feldman, *Electronic Thin Film Science - for Electrical Engineers and Materials Scientists* (Macmillan Publishing Company, New York, 1992), p. 428.
[20] B. H. L. Chao, X. Zhang, S. H. Chae, and P. S. Ho, Microelectron. Reliab. **49**(3), 253 (2009).
[21] T. A. Siewert, J. C. Madeni, and S. Liu, in *Proceedings of the APEX Conference on Electronics Manufacturing, Anaheim, California, April, 2003*.
[22] H. J. Frost and M. F. Ashby, *Deformation-Mechanism Maps* (Oxford, New York, Pergamon Press, Sydney, 1982).
[23] J. R. Rice, in *IUTAM Symposium on 3-D Constitutive Relationship and Ductile Failure*, edited by S. Nemat-Nassar (Martinus Nordhoff, Dordrecht, 1981).
[24] T. Surholt and C. Herzig, Acta Mater. **45**(9), 3817 (1997).
[25] W. H. Safranek, *The Properties of Electrodeposited Metals and Alloys*, 2nd ed. (American Electroplaters and Surface Finishers Society, Orlando, FL, 1986).
[26] Y. Zhou, C. S. Yang, J. A. Chen, G. F. Ding, W. Ding, L. Wang, M. J. Wang, Y. M. Zhang, and T. H. Zhang, Thin Solid Films **460**(1–2), 175 (2004).
[27] M. J. H. Van Dal, A. A. Kodentsov, and F. J. J. Van Loo, Intermetallics **9**(6), 451 (2001).
[28] S. Wiese, A. Schubert, H. Walter, R. Dudek, F. Feustel, E. Meusel, and B. Michel, in *Proceedings of 21st Electronic Components and Technology Conference, 2001*.
[29] S. B. Kim and J. Yu, J. Electron. Mater. **39**(3), 326 (2010).
[30] M. Onishi and H. Fujibuchi, Trans. Jpn. Inst. Met. **16**(9), 539 (1975), available at https://www.jstage.jst.go.jp/article/matertrans1960/16/9/16_9_539/_article.
[31] K. N. Tu and R. D. Thompson, Acta Metall. **30**(5), 947 (1982).
[32] S. Kumar, C. A. Handwerker, and M. A. Dayananda, J. Phase Equilib. Diffus. **32**(4), 309 (2011).
[33] A. Paul, A. A. Kodentsov, and F. J. J. Van Loo, Z. Metallkd. **95**(10), 913 (2004).
[34] A. Paul, C. Ghosh, and W. J. Boettinger, Metall. Mater. Trans. A **42**(4), 952 (2011).
[35] Y. Wang, S. H. Chae, J. Im, and P. S. Ho, in *2013 IEEE 63rd Electronic Components and Technology Conference, ECTC*, Las Vegas, NV (2013), p. 1953.
[36] B. Budiansky, J. W. Hutchinson, and S. Slutsky, in *Mechanics of Solids* (Pergamon Press, Oxford, 1982), p.13.
[37] R. Hill, J. Mech. Phys. Solids **5**(1), 66 (1956).
[38] M. Y. He and J. W. Hutchinson, Trans. ASME J. Appl. Mech. **48**(4), 830 (1981).

[This article is copyrighted as indicated in the article. Reuse of AIP content is subject to the terms at: http://scitation.aip.org/termsconditions. Downloaded to] IP: 143.248.118.104 On: Wed, 21 May 2014 00:20:17